

pubs.acs.org/Macromolecules Article

# Salt Effect on the Viscosity of Semidilute Polyelectrolyte Solutions: Sodium Polystyrenesulfonate

Anish Gulati, Michael Jacobs, Carlos G. Lopez,\* and Andrey V. Dobrynin\*



Cite This: Macromolecules 2023, 56, 2183–2193



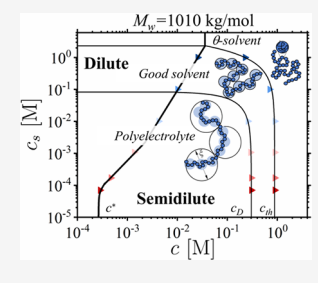
**ACCESS** I

III Metrics & More

Article Recommendations

Supporting Information

**ABSTRACT:** We studied the viscosity of semidilute aqueous solutions of sodium polystyrenesul-fonate as a function of polymer and salt concentrations. The viscosity data were quantified by applying a scaling relationship between solution correlation length  $\xi = lg^{\nu}/B$  and number of monomers g per correlation volume for chains with monomer projection length l. The specific values  $B_{p\varphi}B_{g}$ , and  $B_{th}$  of the B-parameter corresponding to exponents  $\nu = 1$ , 0.588, and 0.5 were determined by the fraction of charged monomers and their degree of ionization, the effective solvent quality for the polymer backbone, the chain Kuhn length, and the type and strength of monomer—solvent interactions. The values of the B-parameters were obtained from the plateaus of normalized specific viscosity  $\eta_{sp}(c)/N_{w}(cl^{3})^{1/(3\nu-1)}$  as a function of the monomer concentration c for polyelectrolytes with weight-average degree of polymerization  $N_{w}$ . The extension of this approach to the entangled solution



regime allowed us to determine the packing number of a chain of correlation blobs,  $\tilde{P}_e$ , which completes the set of parameters  $\{B_{pe}, B_g, B_{th}, \tilde{P}_e\}$  uniquely describing static and dynamic properties of polyelectrolyte solutions. This information was used to construct a diagram of states, calculate the fraction of free counterions and the energy of the electrostatic blobs, and establish a crossover concentration to the entangled solution regime.

# ■ INTRODUCTION

Polyelectrolytes are polymers with ionic groups which find applications as paint, adhesives, or paper<sup>1–4</sup> and medical products.<sup>5</sup> Examples of polyelectrolytes include biological molecules such as DNA, RNA, or hyaluronic acid as well as synthetic ones such as polystyrenesulfonate, carboxymethyl cellulose, or poly(acrylic acid). Solution properties of polyelectrolytes are controlled by the chain degree of polymerization, fraction and distribution of the ionic groups, solvent quality for the polymer backbone, polymer and added salt concentrations, and solution pH.<sup>6–11</sup>

Sodium polystyrenesulfonate (NaPSS) is one of the most studied examples of synthetic polyelectrolytes, owing to the availability of low polydispersity standards covering a wide range of molar masses and an easy control over the degree of sulfonation determining polyelectrolyte solubility in aqueous solutions. 8,9,12-30 After over 40 years of research, it is now well understood that in salt-free solutions of NaPSS strong electrostatic interactions between ionized groups result in a chain stretching which is manifested as a strong dependence of the crossover concentration to a semidilute solution regime  $(c^*)$  on the chain degree of polymerization,  $c^* \propto N^{-2}$ . In the semidilute solution regime  $(c > c^*)$ , electrostatic interactions between charged groups are screened on the length scales beyond the solution correlation length  $\xi \propto c^{-1/2}$ . This strong concentration dependence of the solution correlation length results in the chain size decreasing with increasing polymer concentration as  $R \propto c^{-0.25}$ , which in turn suppresses chain entanglements and broadens the Rouse regime of chain dynamics.31-33 The addition of excess salt exponentially

screens the electrostatic interactions between ionized groups on the polymer backbones such that the polyelectrolyte solutions behave as solutions of neutral polymer with salt-dependent second virial coefficient and chain persistence length. 12,16,17,21,34–50 The degree of sulfonation plays an important role in the solubility of NaPSS such that polyelectrolytes with a degree of sulfonation below 30% become insoluble and precipitate. 22

Despite these efforts, a quantitative understanding of polyelectrolyte solutions of NaPSS is still lacking. To fill this void, we conducted a detailed study of salt effect on the solution properties over a broad range of molecular weights and polymer and salt concentrations. Applying a recently developed quantitative version of the scaling approach based on the analysis of the solution viscosity in the unentangled (Rouse) regime, <sup>12,31,51–53</sup> we determine blob dimensions in the different solution regimes and crossover concentrations between them, the fraction of "free" counterions, the salt concentration dependence of the excluded volume, and the blob packing number defining the onset of entanglements in semidilute polyelectrolyte solutions.

Received: October 17, 2022 Revised: January 9, 2023 Published: February 20, 2023





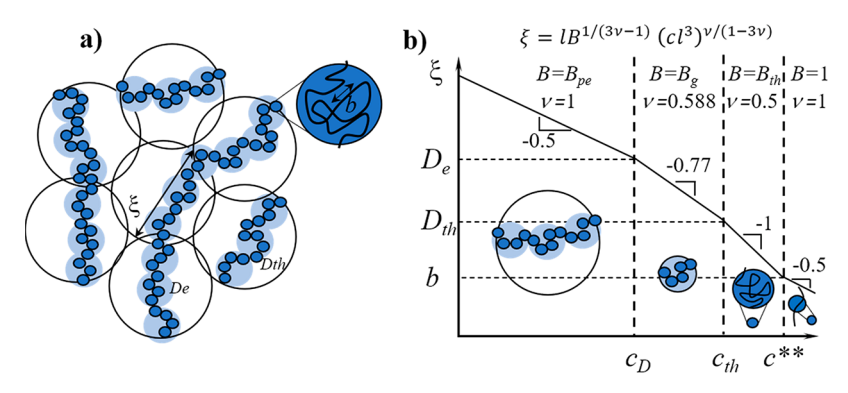


**Figure 1.** (a) Schematic representation of the hierarchy of length scales in semidilute salt-free polyelectrolyte solutions. (b) Concentration dependence of the solution correlation length in salt-free polyelectrolyte solutions for  $c > c^*$ .  $c_D$ , electrostatic blob overlap concentration;  $c_{th}$ , thermal blob overlap concentration; and  $c^{**}$ , crossover concentration to the concentrated solution regime. Insets show chain structure on the length scales of the correlation length. Logarithmic scales. Adapted from ref 12. Copyright ACS 2021.

# MATERIALS AND METHODS

**Materials.** NaPSS for all the molar masses was procured from Polymer Standards Service, USA. The Spectra/Por dialysis membranes with MWCOs of 3.5, 6–8, and 12–15 kDa were purchased from VWR. NaCl (99.9%) was obtained from VWR.

Polymer Purification. The NaPSS was dialyzed against DI water, and the dialysis bath was regularly exchanged until the equilibrium conductivity of the bath stayed below 2  $\mu$ S cm<sup>-1</sup> for at least 6 h. This threshold was determined from the equilibrium conductivity of pure DI water, with an initial conductivity of 0.06  $\mu$ S cm<sup>-1</sup>, presumably due to the formation of carbonic acid on absorption of CO<sub>2</sub> from the atmosphere. 14,40 These dialyses were precautionary to remove any residual ionic impurities. In practice, the purification performed by the vendor was sufficient. The bath conductivity for most of the batches never went above this value, in which case the dialysis was conducted for 24 h. For a few batches, the conductivity went slightly higher to a maximum of 2.6  $\mu$ S cm<sup>-1</sup>. Assuming that the entire increase in conductivity is due to the ionic impurities removed during the dialysis process, the ratio of salt ions to monomers equates to smaller than 1:500. The dialyzed solution was frozen using liquid nitrogen and dried in a freeze-dryer under a vacuum pressure of  $\sim$ 0.4 mbar for 72 to 96 h.

All the measurements reported in this study were performed using freshly dialyzed NaPSS. The NaPSS was recovered after measurements, by dialyzing against DI water. The measurements made using recovered polyelectrolyte, however, were out of trend, possibly due to degradation and were, therefore, repeated using a fresh batch of the polyelectrolyte. In order to confirm that there was no degradation during the measurement, some of the loaded samples were remeasured multiple times without removing them from the instrument. The repeated measurements were found to be in agreement with each other.

**Sample Preparation.** The NaPSS was kept under vacuum for at least 24 h prior to sample preparation to minimize the residual water content. The samples were prepared in polypropylene vials previously washed with DI water and dried in an oven at 60 °C. All the samples were prepared using a weighing balance with a typical error of  $\pm 0.05$  mg. The low-concentration samples were made by dilution with DI water or salt solutions of known concentrations. The densities of the master solutions for dilution were calculated using the known densities of the added components using  $V = m_{NaPSS}/\rho_{NaPSS} + m_{water}/\rho_{water} + m_{NaCI}/\rho_{NaCI}$ . Here, V is the volume in cm<sup>3</sup>, m is the mass in g, and  $\rho$  is the density in g cm<sup>-3</sup>. The densities of NaPSS, water, and NaCl at 25 °C were taken as 1.65, 1, and 2.16 g cm<sup>-3</sup>, respectively. The density of NaPSS has been determined from its partial molar volume in water reported in the literature, <sup>54</sup> which takes into account the effect of solvent on the apparent polymer density.

Static Light Scattering (SLS). The SLS measurements were made using a FICA instrument from Systemtechnik (Denzlingen, Germany). Two lasers with wavelengths,  $\lambda$ , of 407 and 640 nm were

used, and the dn/dc for PS in toluene was taken to be 1.106 and 1.11 mL/g, respectively. <sup>55</sup> The final degrees of polymerization reported are the mean of the two measurements. The measurements were carried out in quartz cuvettes from Hellma Analytics with a diameter of 20 mm. The cuvettes were washed with freshly distilled acetone inside a modified distillation column for at least 30 min before loading the samples. In order to eliminate dust, the samples were filtered using a 0.2  $\mu$ m syringe filter. The instrument was calibrated using toluene as a standard to define the scattering intensity on an absolute scale.

**Rotational Rheometry.** The rotational rheometry was carried out using two stress-controlled rheometers: a Kinexus rheometer from Netzsch and a DHR-3 rheometer from TA Instruments. The Kinexus rheometer was used with cone—plate geometries of two different sizes: a 40 mm plate ( $\theta=1^{\circ}$ , sample volume = 0.3 mL) for high-viscosity samples and a 60 mm plate ( $\theta=2^{\circ}$ , sample volume = 1.97 mL) for the low-viscosity samples. Regular calibrations were carried out using a 20 min torque mapping in air. The DHR-3 rheometer was used with a 40 mm cone—plate geometry ( $\theta=1^{\circ}$ , sample volume = 0.3 mL). Separate torque, inertia, and rotational mappings were performed regularly. A solvent trap filled with DI water was used for all measurements.

**Rolling Ball Viscometry.** A rolling ball microviscometer (Lovis 2000 M from Anton Paar) was used for samples with very low viscosity. The capillary ( $\oplus$  = 1.59 mm) with a lower measurement limit of 0.3 mPa s was used. This instrument utilizes a closed capillary block for the measurements, which prevents evaporation. The measurement principle is based on the calculation of solution dynamic viscosity from the time taken by a steel ball of known density to roll a known distance across the capillary at a certain angle. The instrument was calibrated regularly using a viscosity standard from VWR. The error for this instrument was  $\pm$ 0.5%, as estimated from comparative measurements using a Ubbelohde capillary viscometer. In order to check for shear-thinning, most of the measurements were made as a function of angles between 20° and 70° (steps of 5°) in order to obtain varying shear rates. The shear rates at a given angle can be calculated using the following equations:  $^{56}$ 

$$\dot{\gamma} = \left(\frac{DV}{(D-d)^2}\right) \left(\frac{2(1+n)(1+2n)^2}{n(2+n)(2+3n)}\right) \tag{1}$$

where D is the capillary diameter, d is the ball diameter, V is the ball velocity, and n is the flow behavior index calculated as

$$n = \left(\frac{\log(\sin\theta_1/\sin\theta_2)}{\log(V_1/V_2)}\right) \tag{2}$$

where  $V_1$  and  $V_2$  are the velocities of the rolling ball at angles  $\theta_1$  and  $\theta_2$ , respectively. In some cases, where shear-thinning was not observed for a higher molar mass at a given concentration, the measurements for the lower molar masses were made at a constant angle of 30°.

Table 1. Degree of Polymerization for NaPSS and the Parent PS

	Degree of Polymerization $(N)$									
-	S	odium Polystyi	enesulfonate <sup>b</sup>		Parent Polystyrene					
$M_{w,NaPSS}^{a}$ [kg/mol]	$[\eta]$	SLS	DLS	SANS	GPC <sup>c</sup>	$[\eta]^d$	SLS	PDI <sup>e</sup>	$N_{w,\;Rouse}^{\qquad f}$	
10		70	55	55	50			1.04		
30		140	135	145	151		146	1.06	105	
66	354.5	305	315	280	331	374	348	1.04	230	
150	940	800	800		752	808	885	1.04	525	
271	1605	1700	1350		1354			1.02	1355	
483		2650	2765		2417	2610		1.05	2415	
645					3226			1.07	4140	
1012		4915	6500		5062	5231		1.09	5610	

 $^{a,c,e}$ Provided by Polymer Standard Services.  $^{b}$ Degree of polymerization for NaPSS samples determined by different techniques.  $^{8,67}$   $^{d}N_{w}$  is calculated from MHS given by Fetters et al. for PS in toluene.  $^{66}$   $^{e}$ Polydispersity indices (PDI) calculated as  $M_{w}/M_{n}$  measured using GPC.  $^{f}N_{w}$  is estimated from the analysis of the specific viscosity in the Rouse regime at  $c_{s} = 1.0$  M. The molecular weights can be obtained by multiplying corresponding degrees of polymerizations by 104 and 200 g/mol for precursor and sulfonated polymers, respectively.

**Scaling Analysis.** We applied a scaling approach  $^{12,46,53,57,58}$  to analyze the viscosity of semidilute polyelectrolyte solutions. In the framework of this approach, the correlation length (blob size)  $\xi$  and the number of the repeat units in it, g, with projection length l are related through the general scaling relation  $^{46,57,58}$ 

$$\xi = \lg^{\nu}/B \tag{3}$$

The numerical coefficient B and exponent  $\nu$  are determined by the solvent quality for the polymer backbone and the type and strength of interactions at different length scales starting from the solution correlation length  $\xi$  down to the repeat unit projection length l. In semidilute salt-free polyelectrolyte solutions, the exponent  $\nu=1$ , 0.588, 0.5, and 1, and the B-parameter is equal to  $B_{pe}$ ,  $B_{g}$ ,  $B_{th}$ , and 1 in the different solution concentration regimes, reflecting that correlation blobs are made of electrostatic blobs with sizes  $D_e$  and number of repeat units  $g_e$ , which in turn contain thermal blobs each of size  $D_{th}$  and number of repeat units  $g_{th}$  (Figure 1a).

At the shortest length scales r smaller than the Kuhn length b but larger than or equal to the projection length,  $l \le r < b$ , a section of the chain is rod-like  $(\nu = 1)$  with a linear relationship between the number of repeat units  $g_r$  and its size

$$r = lg_r$$
, for  $l \le r < b$  (4)

This corresponds to the value of B=1. On the length scales smaller than the thermal blob size such that  $b \le r < D_{th}$ , the chain statistics is that of a random walk of Kuhn segments

$$r = (lbg_r)^{0.5} = lg_r^{0.5}/B_{th}, \text{ for } b \le r < D_{th}$$
 (5)

where the parameter

$$B_{th} = (l/b)^{0.5} (6)$$

is always smaller than unity and the exponent  $\nu = 0.5$ .

Excluded volume interactions take over the chain statistics on the length scales  $D_{th} \le r < D_{e^t}$  where the chain statistics is that of a self-avoiding walk of thermal blobs with exponent  $\nu = 0.588$ :

$$r = D_{th}(g_r/g_{th})^{0.588} = lg_r^{0.588}/B_g, \text{ for } D_{th} \le r < D_e$$
 (7)

The parameter  $B_g$  characterizes the degree of swelling of the chain within the electrostatic blob and is related to the repeat unit excluded volume (second virial coefficient)  $\nu$ , Kuhn length b, and projection length l as follows:<sup>40</sup>

$$B_{g} = B_{th} (\nu/(lb)^{1.5})^{1-2\nu}$$
(8)

On the length scales  $D_e \le r < \xi$ , electrostatic repulsion between ionized groups stretches the chain  $(\nu=1)$  such that

$$r = D_{\varrho}g_{r}/g_{\varrho} = \lg_{r}/B_{\varrho\varrho}, \text{ for } D_{\varrho} \le r < \xi$$
(9)

The parameter  $B_{pe}$  is related to the number of repeat units  $g_e$  per electrostatic blob with size  $D_e$ : <sup>12</sup>

$$B_{pe} = lg_{\rho}/D_{e} \tag{10}$$

It is larger than unity and describes the tension in the chain of electrostatic blobs.

The concentration dependence of the solution correlation length  $\xi$  is derived by combining the space-filling condition of correlation blobs:

$$c = g/\xi^3 \tag{11}$$

with scaling relation eq 3. This results in the following expressions for the correlation length:

$$\xi = lB^{1/(3\nu - 1)}(cl^3)^{\nu/(1 - 3\nu)} \tag{12}$$

and the number of chain repeat units per correlation volume:

$$g = B^{3/(3\nu-1)} (cl^3)^{1/(1-3\nu)}$$
(13)

in terms of the *B*-parameters, exponent  $\nu$ , and concentration *c*. Figure 1b illustrates concentration dependence of the solution correlation length in different semidilute solution regimes whose boundaries are defined by  $c_D$ , electrostatic blob overlap concentration,  $c_{th}$ , thermal blob overlap concentration, and  $c^{**}$ , crossover concentration to the concentrated solution regime.

In polyelectrolyte solutions with low salt concentrations, there is an additional screening of the electrostatic interactions on the length scale of correlation blobs by added monovalent salt ions with concentration  $c_g$  which results in the following renormalization of the solution correlation length and number of repeat units in it:  $^{6,46,59}$ 

$$\xi = lB_{pe}^{0.5} (cl^3)^{-0.5} \left( 1 + \frac{2c_s}{f^*c} \right)^{(1-\nu)/(6\nu-2)}$$
(14a)

$$g = B_{pe}^{1.5} (cl^3)^{-0.5} \left( 1 + \frac{2c_s}{f^* c} \right)^{(3-3\nu)/(6\nu-2)}$$
(14b)

where  $f^*$  is the fraction of the free counterions distributed outside the electrostatic blob volume. Equations 14a and 14b are written for an arbitrary exponent  $\nu$  and can be reduced to the familiar form<sup>46</sup> by substituting the Flory exponent  $\nu_F = 0.6$ . At high salt concentrations, the electrostatic interactions are exponentially screened and can be treated as short-range interactions with the  $B_g$ -parameter being salt concentration dependent.

In the framework of the scaling approach it is postulated that the hydrodynamic interactions between chains are screened at the length scale  $\xi_{H}$ , which is proportional to the solution correlation length,  $\xi_{H}\approx\xi_{.}^{57,60-63}$  This assumption results in the solution specific viscosity  $\eta_{sp}$ 

in both the Rouse and entangled solution regimes to be given by the following crossover expression: 12

$$\eta_{sp} = N_w \left( 1 + \frac{N_w}{N_c} \right)^2 \begin{cases} g^{-1}, & \text{for } c \le c^{**} \\ cbl^2, & \text{for } c^{**} < c \end{cases}$$
 (15)

where  $N_w$  is the weight-average degree of polymerization and  $N_e$  is the number of repeat units per entanglement strand, which scales with concentration as follows:  $^{12,64,65}$ 

$$N_{e} = \tilde{P}_{e}^{2} \begin{cases} g, & \text{for } c \leq c^{**} \\ c^{-2}(lb)^{-3}, & \text{for } c^{**} < c \end{cases}$$
 (16)

In eq 16,  $\overline{P_e}$  is the number of entangled strands (packing number) required for a section of a chain with  $N_e$  repeat units to entangle, which also includes information about system polydispersity as explained in refs 12 and 53.

**Degree of Polymerization.** The degree of polymerization of the NaPSS samples and those of the parent polystyrene samples were determined by several techniques. Gel permeation chromatography (carried out by the manufacturer) and SLS and SANS (carried out by us) provide a direct measurement of the molar mass of the polymers, which is translated to a degree of polymerization after dividing by the molar mass of a monomer, set to 200 g/mol for NaPSS, which corresponds to the degree of sulfonation  $\approx$  95%. Estimates of *N* from the diffusion coefficient and intrinsic viscosity are based on Mark–Houwink–Sakurada (MHS) relationships; see refs 8 and 66 for details of their application to the current PSS samples. For the unsulfonated polystyrene we use the MHS relation given by Fetters et al. <sup>66</sup> The results from various techniques are listed in Table 1.

Viscosity Measurements. Viscosity measurements were made in aqueous solutions of NaPSS with  $M_w = 30$ , 271, 483, and 1010 kg/ mol at different polymer and added salt concentrations. The data acquired with the Kinexus and DHR-3 rheometers agreed to within about 5% of each other, with the former generally providing slightly higher viscosities. The measurements from DHR-3 are considered to be more accurate owing to its higher sensitivity and lower torque limit. These aspects help to obtain a wider Newtonian plateau in the low-shear regime, thus providing a more accurate estimate of the zeroshear viscosity  $(\eta(0))$ . Measurements for  $\eta(0)$  in DI water for some of the polymers were reported in earlier publications.<sup>8,68</sup> These results are combined with current measurements; see the SI for additional information. The LOVIS was used to make measurements for samples with viscosities lower than or close to the limit for either rheometer. All the data, along with the instrument used, are provided in the SI. Representative viscosity vs shear rate curves for the 1010 kg/mol polymer are shown in Figure 2 for  $c_s = 0.1$  M and different polymer concentrations. The zero-shear rate viscosity is obtained by averaging the values in the Newtonian plateau at low shear rates.

# ■ RESULTS AND DISCUSSION

We begin with the analysis of polyelectrolyte solution viscosity at different polymer and salt concentrations to quantify the effect of the electrostatic interactions. Figure 3 shows typical  $\eta_{sp}$  vs c curves for NaPSS with  $M_w = 30$ , 271, 483, and 1010 kg/mol at different concentrations of added salt. The maximum measured concentration c was 2 M, and the lower limit was determined by a crossover to the dilute regime at the overlap concentration  $(c^*)$ , which is estimated as  $\eta_{sp} = 1$  ( $\eta_{sp} = (\eta(0) - \eta_s)/\eta_s$ , where  $\eta_s$  is the solvent viscosity and  $\eta(0)$  is the zeroshear viscosity determined from the Newtonian plateau as illustrated in Figure 2). The effective solvent viscosity in solutions of NaCl was obtained from the data of Kestin et al. 69

There are three characteristic regimes of the concentration dependence of solution specific viscosity in Figures 3. At low polymer and salt concentrations for polyelectrolytes with  $M_w = 271 \text{ kg/mol}$  and higher, the specific viscosity first increases

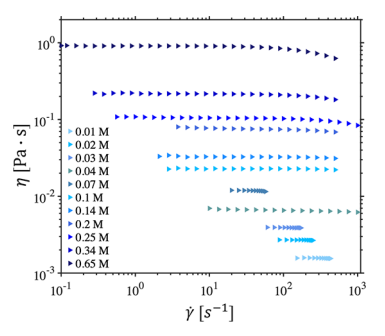


**Figure 2.** Shear rate dependence of the solution viscosity in aqueous solutions of NaPSS with  $M_w = 1010$  kg/mol at salt concentration  $c_s = 0.1$  M and different monomer concentrations as indicated in the legend. The four flow curves with limited shear rate range (c = 0.01, 0.02, 0.03, and 0.07 M) are measured with a LOVIS viscometer, and the rest are measured with the DHR rheometer.

with polymer concentration as  $\eta_{sp} \propto c^{1.31}$ , which is a characteristic feature of semidilute polymer solutions of neutral polymers in a good solvent for the polymer backbone. This reflects the dominant role of salt ions in screening the electrostatic interactions on the length scales of the solution correlation length,  $\xi$ . The observed scaling relationship immediately follows from the expression for the number of chain repeat units per correlation volume (eq 14bb) and the linear scaling of the solution specific viscosity with the number of correlation blobs per chain  $(\eta_{sp} = N_w/g)$  in the Rouse regime. After some algebra we arrive at

$$\eta_{sp} \propto N_{w} c^{1.31} c_{s}^{-0.81}$$
(17)

Thus, the addition of salt decreases solution viscosity and broadens the salt-dominated screening regime. Note that this behavior is even observed for salt-free systems, indicating the presence of a residual salt in DI water samples. With increasing polymer concentration, we observe a crossover to the classical polyelectrolyte regime with  $\eta_{sp} \propto c^{0.5.70,71}$  This is followed by a regime with  $\eta_{sp} \propto c^{1.31}$  corresponding to a solution of overlapping electrostatic blobs  $(c > c_D)$  where electrostatic interactions are screened by counterions and charges on the polymer chains such that solution properties are similar to those in semidilute solutions of neutral polymers. At even higher polymer concentrations, there is a stronger concentration dependence of the solution viscosity, which could be attributed either to the crossover to the concentrated solution regime  $(c > c^{**})$  or to the onset of entanglements. We will come back to this issue below.

At salt concentrations  $c_s \ge 0.01$  M, we observe  $\eta_{sp} \propto c^{1.31}$  scaling in the entire semidilute solution regime. This points out the complete screening of the electrostatic interactions by salt ions. For such salt concentrations, polyelectrolytes behave as neutral polymers with salt-dependent second virial coefficient and chain persistence length. This is confirmed by a systematic decrease of the solution viscosity at the same polymer concentration as the salt content increases.

Having established the existence of different solution regimes, we can use the approach developed in refs 12, 31, and 51–53 and briefly described in the Methods section to obtain the corresponding numerical values of the *B*-parameters (Figure 1b) and use this information to estimate blob dimensions and crossover concentrations between different solution regimes (Table 2). The approach takes advantage of the linear relationship between solution specific viscosity and

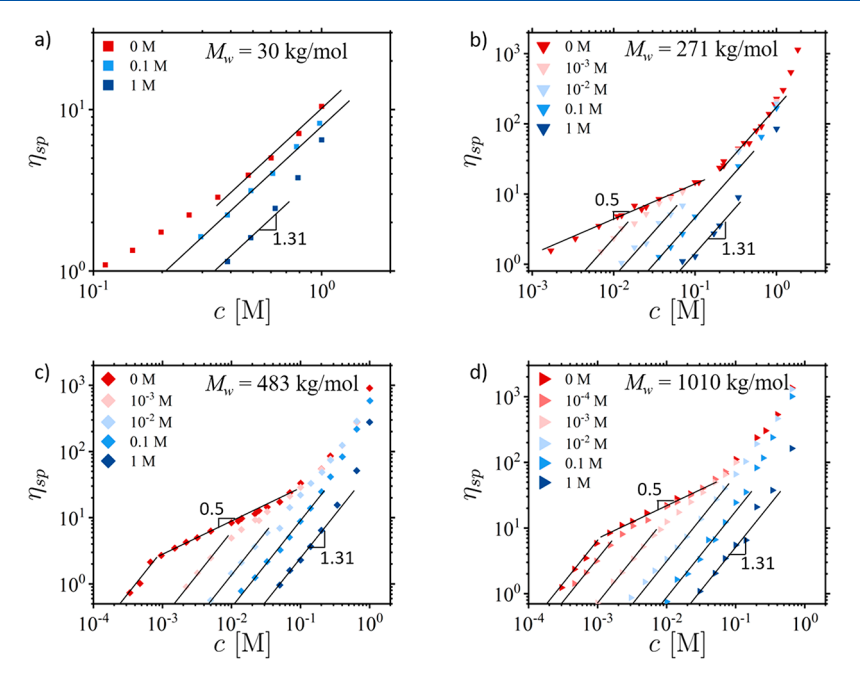


Figure 3. Concentration dependence of specific viscosity ( $\eta_{sp}$ ) in polyelectrolyte solutions of NaPSS with  $M_w = 30$  kg/mol (a), 271 kg/mol (b), 483 kg/mol (c), and 1010 kg/mol (d) at different added salt concentrations of NaCl. Logarithmic scales.

number of correlation blobs per chain in the Rouse regime which immediately follows from the crossover expression eq 15 by setting  $N_w/N_e \ll 1$ . Thus, by using the concentration dependence of g given by eqs 13 and 14b, we obtain B-values from the plateau values  $C_p$  of the normalized solution viscosity  $\eta_{sp}/N_w(cl^3)^{1/(3\nu-1)}$  as a function of concentration using the corresponding exponent  $\nu$  in the different solution regimes (see Figure 1b).

In the so-called polyelectrolyte regime where electrostatic interactions induce chain stretching on the length scales of the solution correlation length such that exponent  $\nu=1$  and the concentration-dependent normalization factor is  $(cl^3)^{0.5}$ . This is illustrated in Figure 4a, where data for polyelectrolyte solutions of chains with different degrees of polymerizations have collapsed defining location of the plateau shown by the dashed line. From this plateau value we calculate  $B_{pe}=C_p^{-2/3}=2.09$ , which is consistent with  $B_{pe}=1.5-1.8$  obtained from the SANS/SAXS measurements of the correlation length in aqueous salt-free solutions of NaPSS. 8,9,25,72,73 Note that the difference between viscosity and SAXS/SANS-based values of  $B_{pe}$  is due to selected normalization. In the viscosity approach,  $\eta_{sp}=N_w/g=N_wB_{pe}^{-3/2}(cl^3)^{1/2}$ , while in scattering  $\xi q^*=q^*lB_{pe}^{1/2}(cl^3)^{-1/2}=2\pi$ .

Values of the  $B_g$ -parameters at different salt concentrations are determined by plotting  $\eta_{sp}/N_w(cl^3)^{1.31}$  as a function of the monomer concentration where we substituted  $\nu=0.588$  to obtain exponent  $1/(3\nu-1)=1.31$  (Figure 4b and c). The plateau values, shown by the dashed lines, monotonically decrease with increasing salt concentration (see eq 17), which is consistent with a decrease of the effective excluded volume representing the strength of the electrostatic interactions. The existence of the plateau even in the salt-free solutions (Figure 4b) points out the presence of residual salt in the DI samples. Using plateau values in Figure 4b and c, we calculate  $B_{g,eff}=C_p^{1/3-0.588}$  and  $B_g=C_p^{1/3-0.588}$ , respectively (Table 2). The values of  $B_{g,eff}$  (Figure 4b) describe screening of the electrostatic interactions on the length scales larger than the electrostatic blob size, while  $B_g$ -parameters obtained from Figure 4c

characterize properties of the polymer backbone at short-length scales and quantify the effective solvent quality and Kuhn length (see eq 8).

At high salt concentrations ( $c_s = 0.1-1$  M), the screening by salt ions reduces electrostatic interactions between ionized groups on the polymer backbones to the short-range interactions with salt concentration dependent excluded volume. In this salt concentration range, polyelectrolytes behave as neutral polymers in a marginally good solvent. We use normalized viscosity data at  $c_s = 0.1$  M and  $c_s = 1$  M to adjust the provided values of the weight-average degree of polymerization  $N_w$  by achieving a collapse of the plateaus for samples with different molecular weights (Table 2). For this molecular weight correction, samples with 271 and 483 kg/mol were used as molecular weight standards since their normalized viscosity data overlap in the plateau region without requiring a correction.

The plateau values in Figure 4b for the salt-free and low-salt concentrations allow us to estimate the residual salt concentration  $c_{s,res} \approx 7.4 \times 10^{-5}$  M and fraction of free counterions  $f^* \approx 0.16$  for  $c_s < 0.01$  M and  $f^* \approx 0.19$  for  $c_s = 0.01$  M by taking into account that in the salt-dominated regime (see eq 14)

$$g = B_{pe}^{1.5} (cl^3)^{1/(1-3\nu)} \left( \frac{2(c_s + c_{s,res})l^3}{f^*} \right)^{(3-3\nu)/(6\nu-2)}$$

$$= B_{g,eff}^{3/(3\nu-1)} (cl^3)^{1/(1-3\nu)}$$
(18)

where  $B_{g,eff}$  corresponds to a low-c plateau in Figure 4b and solving eq 18 for the ratio

$$\frac{(c_s + c_{s,res})}{f^*} = \frac{1}{2l^3} B_{pe}^{(3\nu - 1)/(\nu - 1)} B_{g,eff}^{2/(1-\nu)}$$
(19)

at different salt concentrations,  $c_s$ . The estimated values of  $f^*$  are consistent with osmotic pressure and conductivity measurements, which yield  $f^* \approx 0.2$ . Note that a similar

Table 2. Summary of Scaling Parameters

		,														
$M_{\nu}  [\mathrm{kg/mol}]$	$M_{\nu}  [\mathrm{kg/mol}] $	$c_s$ [M]	$B_{pe}$	$B_{geff}$	$B_g$	$B_{th}$	$c_D^a$ [M]	$c_{th}^{b}$ [M]	$c^{**c}$ [M]	$c_e^d$ [M]	se e	$D_e^e$ [nm]	Sth	$D_{th}^{f}$ [nm]	<i>b</i> <sup>g</sup> [nm]	$v^{h}$ [nm <sup>3</sup> ]
30	21	0	2.09(17)	0.122(2)	0.402(7)	0.320(4)	0.305	0.895	1.05	3.96	55	69.9	13	2.92	2.49	0.138
		0.1			0.419(10)	0.320(4)		0.707	1.05	3.96			21	3.70	2.49	0.109
		П			0.573(29)	0.344(6)		0.227	1.41	4.93			323	13.31	2.15	0.023
99	46	0	2.09(17)	0.122(2)	0.402(7)	0.320(4)	0.305	0.895	1.05	3.47	55	69.9	13	2.92	2.49	0.138
150	105	0	2.09(17)	0.122(2)	0.402(7)	0.320(4)	0.305	0.895	1.05	3.03	55	69.9	13	2.92	2.49	0.138
		0.01	1.90(12)	0.311(4)	0.402(7)	0.320(4)	0.366	0.895	1.05	3.03	43	5.81	13	2.92	2.49	0.138
		0.1			0.419(10)	0.320(4)		0.707	1.05	3.03			21	3.70	2.49	0.109
		1			0.573(29)	0.344(6)		0.227	1.41	3.77			323	13.31	2.15	0.023
271	271	0	2.09(17)	0.122(2)	0.402(7)	0.320(4)	0.305	0.895	1.05	2.58	55	69.9	13	2.92	2.49	0.138
		0.001	2.09(17)	0.212(2)	0.402(7)	0.320(4)	0.305	0.895	1.05	2.58	55	69.9	13	2.92	2.49	0.138
		0.01	1.90(12)	0.311(4)	0.402(7)	0.320(4)	0.366	0.895	1.05	2.58	43	5.81	13	2.92	2.49	0.138
		0.1			0.419(10)	0.320(4)		0.707	1.05	2.58			21	3.70	2.49	0.109
		1			0.573(29)	0.344(6)		0.227	1.41	3.22			323	13.31	2.15	0.023
483	483	0	2.09(17)	0.122(2)	0.402(7)	0.320(4)	0.305	0.895	1.05	2.35	55	69.9	13	2.92	2.49	0.138
		0.001	2.09(17)	0.212(2)	0.402(7)	0.320(4)	0.305	0.895	1.05	2.35	55	69.9	13	2.92	2.49	0.138
		0.01	1.90(12)	0.311(4)	0.402(7)	0.320(4)	0.366	0.895	1.05	2.35	43	5.81	13	2.92	2.49	0.138
		0.1			0.419(10)	0.320(4)		0.707	1.05	2.35			21	3.70	2.49	0.109
		1			0.573(29)	0.344(6)		0.227	1.41	2.93			323	13.31	2.15	0.023
645	828	1			0.573(29)	0.344(6)		0.227	1.41	2.67			323	13.31	2.15	0.023
1010	1122	0	2.09(17)	0.122(2)	0.402(7)	0.320(4)	0.305	0.895	1.05	2.04	55	69.9	13	2.92	2.49	0.138
		0.0001	2.09(17)	0.145(1)	0.402(7)	0.320(4)	0.305	0.895	1.05	2.04	55	69.9	13	2.92	2.49	0.138
		0.001	2.09(17)	0.212(2)	0.402(7)	0.320(4)	0.305	0.895	1.05	2.04	55	69.9	13	2.92	2.49	0.138
		0.01	1.90(12)	0.311(4)	0.402(7)	0.320(4)	0.366	0.895	1.05	2.04	43	5.81	13	2.92	2.49	0.138
		0.1			0.419(10)	0.320(4)		0.707	1.05	2.04			21	3.70	2.49	0.109
		1			0.573(29)	0.344(6)		0.227	1.41	2.54			323	13.31	2.15	0.023
				, ,,,,,,,,,,,,,,,,,,,,,,,,,,,,,,,,,,,,,	4									,		

12, respectively, for  $B=B_g$  and  $\nu=0.588$ . fCalculated with eqs 13 and 12, respectively, for  $B=B_h$  and  $\nu=0.5$ .  $gb=1B_{h}^{-2}$  (see eq 6).  $hv=(1b)^{1.5}(B_{hb}/B_g)^{1/(2\nu-1)}$  (see eq 8). The numbers in parentheses . "Calculated with eqs 13 and are the uncertainties of the respective values of the B-parameters to the precision of the same number of least significant digits, evaluated as  $\sigma_{\rm B} = \left(\nu - \frac{1}{3}\right)\sigma_{\rm C}B/C_p$ , where  $C_p$  is the average plateau value,  $=B_g^{3/(3\nu-1)}(c_Dl^3)^{1/(1-3\nu)}\cdot c_{th}l^3=B_h^3(B_{th}/B_g)^{1/(2\nu-1)}\cdot c_**\beta=B_{th}^4\cdot {}^4\mathrm{Calculated\ as\ } c_\varepsilon=\frac{B_{th}^3}{l^3}\binom{P_c^2}{N_w}^{\nu-1/3}.$  $\sigma_{\rm C}$  is the uncertainty in the plateau value corresponding to one standard deviation, and  $B=C_p^{1/3u}$  $^a\mathrm{Calculated} \text{ by numerically solving } B^{1.5}_{pe}(c_D l^3)^{-0.5} \bigg(1 + \frac{2\epsilon_c}{l^4 c_0}\bigg)^{(3-3\nu)/(6\nu-2)}:$ 

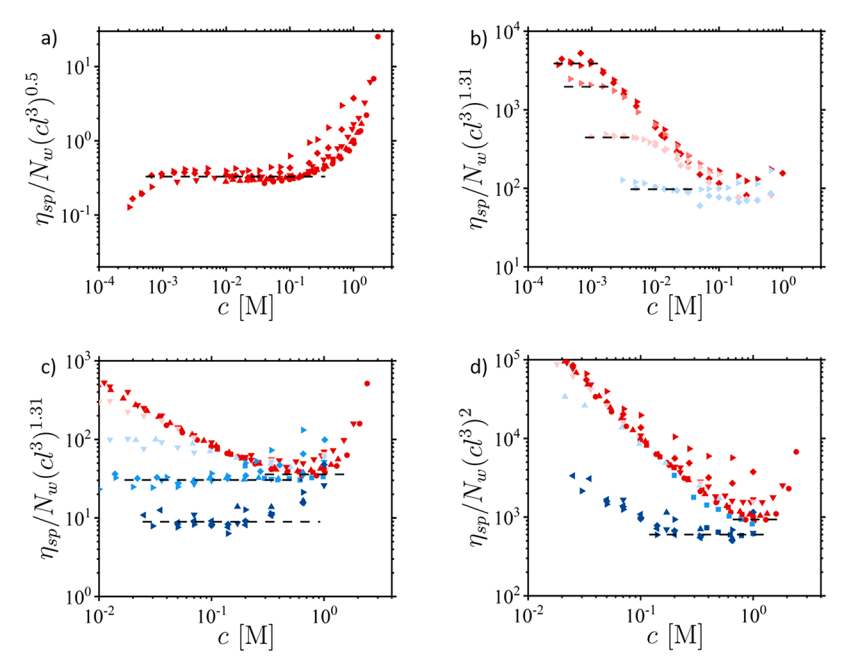


Figure 4. Dependence of the normalized specific viscosity  $\eta_{sp}/N_w(cl^3)^{0.5}$  (a),  $\eta_{sp}/N_w(cl^3)^{1.31}$  (b and c), and  $\eta_{sp}/N_w(cl^3)^2$  (d) on polymer concentration in polyelectrolyte solutions of NaPSS with  $M_w = 30$  kg/mol (squares), 66 kg/mol (circles), 150 kg/mol (up triangles), 271 kg/mol (down triangles), 483 kg/mol (rhombs), 645 kg/mol (left triangles), and 1010 kg/mol (right triangles) at different salt concentrations. Panel (b) only shows data for  $M_w = 483$  and 1010 kg/mol at salt concentrations  $c_s \le 0.01$  M. Panel (c) shows the rest of the data for  $\eta_{sp}/N_w(cl^3)^{1.31}$  with only high concentration plateaus corresponding to the  $B_g$ -parameter being highlighted. The degree of polymerization for these plots was corrected to overlap data at  $c_s = 1$  M (Table 2) as described in the text,  $N_w$  is calculated with  $M_0 = 200$  g/mol and l = 0.255 nm is the monomer projection length. Dashed lines show corresponding plateau locations,  $C_p$ . Symbol notations are the same as in Figure 3. Logarithmic scales.

result can be obtained from location of the maximum in the  $\eta_{sp}(c)/c$  plot. The calculated value of  $c_{s,res}$  is close to the value of  $2 \times 10^{-4}$  M obtained by Han et al. <sup>14</sup> from conductivity measurements of CsPSS in salt-free aqueous solutions.

Finally, we calculate  $B_{th}$  by plotting  $\eta_{sp}/N_w$  ( $cl^3$ )<sup>2</sup> vs c (Figure 4d). This gives  $B_{th}=0.320$  for  $c_s \leq 0.1$  M and  $B_{th}=0.344$  for  $c_s=1$  M The corresponding Kuhn lengths of the backbones are b=2.49 nm and b=2.15 nm, respectively. This indicates that polyelectrolytes become more flexible at the highest salt concentration  $c_s=1$  M. These Kuhn length values are close to the bare Kuhn length of NaPSS 2.2 nm estimated in previous studies. Note that the upturn in the data at high concentrations corresponds to crossover to a solution of entangled chains, which is consistent with an observed strong dependence on the degree of polymerization.

Information about the electrostatic blob size and the number of monomers in it, summarized in Table 2, can be used for the evaluation of the electrostatic energy of a blob in terms of the thermal energy  $k_BT$  for low salt concentrations ( $c_s < 0.01$  M).

$$U_{blob} \approx nk_{\rm B}T \approx k_{\rm B}Tl_{\rm B} \frac{(g_{\rm e}f^*)^2}{D_{\rm e}} \tag{20}$$

where  $l_B \approx 0.7$  nm is the Bjerrum length in water at normal conditions. Taking into account  $f^* \approx 0.16$ , we estimate the electrostatic energy per blob to be  $8.1k_BT$ . Note that the large value of the blob energy is a result of including all numerical coefficients into the blob definitions by setting  $N_w \approx g$  at the overlap concentration  $(\eta_{sp}(c^*) = 1)$  and in eq 11 defining the concentration dependence of blobs.

The Manning counterion condensation parameter 75,76 for such electrostatic blobs is equal to

$$\frac{l_{\rm B}g_{\rm e}f^*}{D_{\rm e}}\approx 0.92\tag{21}$$

This value is close to unity, which is usually used to estimate the counterion condensation threshold. Thus, counterions localized inside an electrostatic blob reduce the energy of electrostatic attraction of a free counterion on the blob surface to approximately  $-0.92k_BT$ .

We can estimate the fraction of free counterions  $f^*$  by using the value of  $B_{pe} = 2.09$  and its definition (eq 10) and setting the Manning counterion condensation parameter  $^{76,77}$  to unity. This gives  $f^* \approx 0.17$ , which is close to the value obtained from the viscosity data. In the framework of this approximation, the energy of the electrostatic blob in terms of the thermal energy  $k_BT$  is calculated as the ratio of the electrostatic blob size  $D_e$  and the Bjerrum length  $l_B$  such that  $U_{blob} \approx k_BTD_e/l_B \approx 9.6k_BT$ , which immediately follows from eq 20. This value is about 15% larger than the one evaluated directly from blob dimensions but still provides a reasonable estimate. Thus, the outlined approach could be implemented for calculations of the electrostatic energy of a blob and  $f^*$  for polyelectrolyte systems where it cannot be directly determined from the viscosity data.

Figure 5 shows the dependence of the excluded volume ( $\nu$ ) on the salt concentration in different solution regimes. The values of  $c_s$  are calculated by adding up added salt and residual salt concentrations, using the estimated value of  $c_{s,res} \approx 7.4 \times 10^{-5}$  M. The black square corresponds to the  $\theta$  conditions ( $\nu$  = 0) reported by Takahashi et al. for NaPSS in 4.17 M NaCl at 25 °C. The excluded volume first remains constant then begins to decrease with increasing salt concentration when the Debye screening length becomes smaller than electrostatic blob size, indicating changes in the backbone solvation and

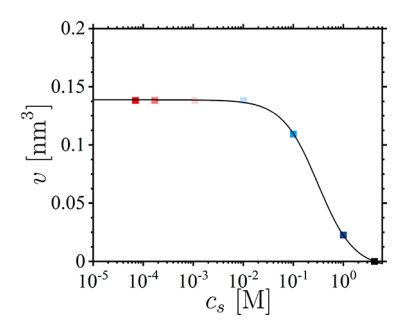


**Figure 5.** Dependence of the excluded volume on the salt concentration in NaPSS solutions. The values of  $c_s$  are calculated taking into account a residual salt concentration of  $7.4 \times 10^{-5}$  M. Colored points are from Table 2, and the black square marks the Takahashi et al.<sup>20</sup>  $\theta$  point at 4.17 M. Solid line is an interpolation spline.

exponential screening of the electrostatic interactions on length scales smaller than the electrostatic blob size where the chain statistics is determined by the polymer—solvent affinity.

Using the results of the specific viscosity analysis in the different solution regimes together with corresponding cross-over concentrations (Table 2), we can replot all viscosity data in the universal form (Figure 6) and fit the data to determine a

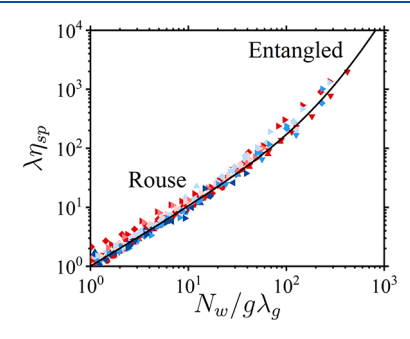


**Figure 6.** Universal representation of the solution specific viscosity as a function of the number of correlation blobs per polyelectrolyte chain

$$N_w/g$$
. The solid line is the best fit to  $\lambda \eta_{sp} = \frac{N_w}{g\lambda_g^2} \left(1 + \frac{N_w}{p_c^2 g\lambda_g^2}\right)^2$  with  $\widetilde{P_c} = 18$  with normalization factors  $\lambda_g = 1$  for  $c \le c^{**}$  and  $\lambda_g = (c/c^{**})^{-1.5}$  for  $c > c^{**}$ ;  $\lambda = 1$  for  $c \le c^{**}$  and  $\lambda = c/c^{**}$  for  $c > c^{**}$ . Symbol notations are the same as in Figure 3.

packing number,  $\overline{P_e} = 18$ . There are two well-defined scaling regimes. At a small number of correlation blobs per chain, we recover the linear scaling of  $\eta_{sp} = N_w/g$ , corresponding to the Rouse regime. When the number of correlation blobs per chain exceeds ~350, there is a crossover to the entangled solution regime with  $\overline{P_e} = 18$ . The crossover concentration to the entangled solution regime  $c_e$  (Table 2) is estimated by setting  $N_w \approx N_e$ , whose concentration dependence and relation to the packing parameter are given by eq 16. For all systems it is in the concentrated solution regime,  $c_e > c^{**}$ . Note that with increasing salt concentration beyond  $c_s = 1$  M one should expect a crossover to a  $\theta$ -solvent regime (see Figure 5), where entanglement molecular weight is determined by the Colby—Rubinstein conjecture.

Figure 7 summarizes our results by showing the diagram of states of different solution regimes calculated using data in Table 2 for samples with  $M_{\rm w}=1010$  kg/mol. There are two characteristic scaling regimes describing the crossover to

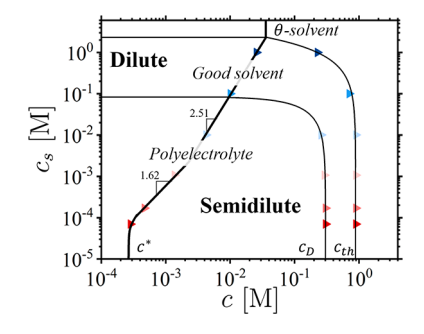


Figure 7. Diagram of states of different solution regimes for NaPSS with  $M_w = 1010$  kg/mol. Solid lines represent crossovers between different regimes with  $c_D$  and  $c_{th}$  pointing out crossovers between polyelectrolyte, good, and θ-solvent solutions, respectively.

semidilute polyelectrolyte solutions. Crossover to the semidilute solution regime for  $c_s < 0.01$  M is given by  $c_s^* \propto (c^*)^{1.62}$ , which immediately follows from eq 17 by setting  $\eta_{sp} \approx 1$ . For high salt concentration, we observe  $c_s^* \propto (c^*)^{2.51}$ . This scaling follows from the salt dependence of the  $B_g$ -parameter,  $B_g \propto c_s^{0.133}$ , which accounts for the variation of both the excluded volume  $\nu$  and Kuhn length with the salt concentration (see eq 8). At high salt or polymer concentrations, their effect of the electrostatic interactions reduces to changes in the solvent quality for the polymer backbone and its Kuhn length (good and  $\theta$ -solvent regimes). This takes place above the concentration of overlapping electrostatic blobs.

# CONCLUSIONS

We have studied the effect of salt concentration on the viscosity of semidilute polyelectrolyte solutions. By applying a scaling approach, we have determined the solution correlation length, chain interaction parameters, and Kuhn length and established their dependences on the polymer and salt concentrations. In particular, we have calculated blob sizes and number of monomers in them in different solution regimes and corresponding crossover concentrations (Table 2). The unexpected result is that a crossover to the semidilute solution regime for polyelectrolytes with high molecular weights takes place at polymer concentrations where residual and added salt dominate the screening of electrostatic interactions. In this salt concentration regime, analysis of the viscosity data has allowed us to decouple contribution of residual salt and fraction of ionized group into the solution correlation length, providing a means for their estimate, and use this information to calculate the counterion condensation parameter and blob electrostatic energy (eqs 18 and 19). By representing viscosity data in terms of the number of correlation blobs per chain (Figure 6), we have shown that polyelectrolyte chains entangle at monomer concentrations above the crossover concentration to the concentrated solution regime for the studied range of degrees of polymerization. A linear scaling of the solution viscosity with the degree of polymerization in the Rouse regime offers a new way to determine the weight-average molecular weight (Table 2). Furthermore, the obtained information is used to construct a diagram of states of polyelectrolyte solutions (Figure 7) and to predict solution properties at different salt and polymer concentrations. We hope that the developed approach will become a useful tool for the quantitative analysis of other polyelectrolyte systems.

### ASSOCIATED CONTENT

# **5** Supporting Information

The Supporting Information is available free of charge at https://pubs.acs.org/doi/10.1021/acs.macromol.2c02128.

Viscosity data sets (XLSX)

### AUTHOR INFORMATION

### **Corresponding Authors**

Andrey V. Dobrynin — Department of Chemistry, University of North Carolina at Chapel Hill, Chapel Hill, North Carolina 27599-3290, United States; oorcid.org/0000-0002-6484-7409; Email: avd@email.unc.edu

Carlos G. Lopez — Institute of Physical Chemistry, RWTH Aachen University, Aachen 52056, Germany; Email: lopez@pc.rwth-aachen.de

#### Authors

Anish Gulati — Institute of Physical Chemistry, RWTH Aachen University, Aachen 52056, Germany; ⊙ orcid.org/ 0000-0003-2312-5634

Michael Jacobs — Department of Chemistry, University of North Carolina at Chapel Hill, Chapel Hill, North Carolina 27599-3290, United States; Center for Nanophase Materials Sciences, Oak Ridge National Laboratory, Oak Ridge, Tennessee 37830, United States; orcid.org/0000-0002-7255-3451

Complete contact information is available at: https://pubs.acs.org/10.1021/acs.macromol.2c02128

#### Notes

The authors declare no competing financial interest.

# ACKNOWLEDGMENTS

This work was supported by the DFG, project GO 3250/2-1 (A.G. and C.G.L.), and by the National Science Foundation under the Grants DMREF-2049518 and 1921923 (A.V.D. and M.J.). The authors are grateful to Prof. Ralph Colby for stimulating discussions.

# REFERENCES

- (1) Durmaz, E. N.; Sahin, S.; Virga, E.; de Beer, S.; de Smet, L. C. P. M.; de Vos, W. M. Polyelectrolytes as Building Blocks for Next-Generation Membranes with Advanced Functionalities. *ACS Appl. Polym. Mater.* **2021**, 3 (9), 4347–4374.
- (2) Khan, A.; Ubaid, F.; Fayyad, E. M.; Ahmad, Z.; Shakoor, R. A.; Montemor, M. F.; Kahraman, R.; Mansour, S.; Hassan, M. K.; Hasan, A.; et al. Synthesis and properties of polyelectrolyte multilayered microcapsules reinforced smart coatings. *J. Mater. Sci.* **2019**, *54* (18), 12079–12094.
- (3) Lee, J.; Hye Jung, Y. Strengthening effect of polyelectrolyte multilayers on highly filled paper. *Nord Pulp Paper Res. J.* **2018**, 33 (1), 113–121.
- (4) BeMiller, J. N.; Whistler, R. L. Industrial Gums: Polysaccharides and Their Derivatives; Academic Press, 2012.
- (5) Taber, L.; Umerska, A. Polyelectrolyte complexes as nanoparticulate drug delivery systems. *Eur. Pharm. Rev.* **2015**, 20 (3), 36–40.
- (6) Dobrynin, A. V.; Rubinstein, M. Theory of polyelectrolytes in solutions and at surfaces. *Prog. Polym. Sci.* **2005**, *30* (11), 1049–1118.
- (7) Jimenez, L. N.; Martínez Narváez, C. D.; Sharma, V. Solvent Properties Influence the Rheology and Pinching Dynamics of Polyelectrolyte Solutions: Thickening the Pot with Glycerol and Cellulose Gum. *Macromolecules* **2022**, *55* (18), 3432–3451.

- (8) Lopez, C. G.; Linders, J.; Mayer, C.; Richtering, W. Diffusion and Viscosity of Unentangled Polyelectrolytes. *Macromolecules* **2021**, 54 (17), 8088–8103.
- (9) Lopez, C. G.; Richtering, W. Conformation and dynamics of flexible polyelectrolytes in semidilute salt-free solutions. *J. Chem. Phys.* **2018**, *148* (24), 244902.
- (10) Dou, S.; Colby, R. H. Charge density effects in salt-free polyelectrolyte solution rheology. *J. Polym. Sci., Part B: Polym. Phys.* **2006**, 44 (14), 2001–2013.
- (11) Matsumoto, A.; Yoshizawa, R.; Urakawa, O.; Inoue, T.; Shen, A. Q. Rheological Scaling of Ionic Liquid-Based Polyelectrolytes in the Semidilute Unentangled Regime from Low to High Salt Concentrations. *Macromolecules* **2021**, *54* (12), 5648–5661.
- (12) Dobrynin, A. V.; Jacobs, M. When Do Polyelectrolytes Entangle? *Macromolecules* **2021**, *54* (4), 1859–1869.
- (13) Balding, P.; Borrelli, R.; Volkovinsky, R.; Russo, P. S. Physical Properties of Sodium Poly(styrene sulfonate): Comparison to Incompletely Sulfonated Polystyrene. *Macromolecules* **2022**, *55* (5), 1747–1762.
- (14) Han, A.; Uppala, V. V. S.; Parisi, D.; George, C.; Dixon, B. J.; Ayala, C. D.; Li, X.; Madsen, L. A.; Colby, R. H. Determining the Molecular Weight of Polyelectrolytes Using the Rouse Scaling Theory for Salt-Free Semidilute Unentangled Solutions. *Macromolecules* **2022**, *55* (16), 7148–7160.
- (15) Pavlov, G. M.; Okatova, O. V.; Gubarev, A. S.; Gavrilova, I. I.; Panarin, E. F. Strong linear polyelectrolytes in solutions of extreme concentrations of one-one valent salt. Hydrodynamic study. *Macromolecules* **2014**, *47* (8), 2748–2758.
- (16) Iwamoto, Y.; Hirose, E.; Norisuye, T. Electrostatic contributions to chain stiffness and excluded-volume effects in sodium poly (styrenesulfonate) solutions. *Polym. J.* **2000**, 32 (5), 428–434.
- (17) Yashiro, J.; Norisuye, T. Excluded-volume effects on the chain dimensions and transport coefficients of sodium poly (styrene sulfonate) in aqueous sodium chloride. *J. Polym. Sci., Part B: Polym. Phys.* **2002**, 40 (23), 2728–2735.
- (18) Balding, P.; Cueto, R.; Russo, P. S.; Gutekunst, W. R. Synthesis of perfectly sulfonated sodium polystyrene sulfonate over a wide molar mass range via reversible-deactivation radical polymerization. *J. Polym. Sci., Part A: Polym. Chem.* **2019**, *57* (14), 1527–1537.
- (19) Sen, A. K.; Roy, S.; Juvekar, V. A. Effect of structure on solution and interfacial properties of sodium polystyrene sulfonate (NaPSS). *Polym. Int.* **2007**, *56* (2), 167–174.
- (20) Takahashi, A.; Kato, T.; Nagasawa, M. The second virial coefficient of polyelectrolytes. *J. Phys. Chem.* **1967**, *71* (7), 2001–2010.
- (21) Hirose, E.; Iwamoto, Y.; Norisuye, T. Chain stiffness and excluded-volume effects in sodium poly (styrenesulfonate) solutions at high ionic strength. *Macromolecules* **1999**, 32 (25), 8629–8634.
- (22) Spiteri, M.; Williams, C.; Boué, F. Pearl-necklace-like chain conformation of hydrophobic polyelectrolyte: a SANS study of partially sulfonated polystyrene in water. *Macromolecules* **2007**, *40* (18), 6679–6691.
- (23) Kassapidou, K.; Jesse, W.; Kuil, M. E.; Lapp, A.; Egelhaaf, S.; van der Maarel, J. R. C. Structure and Charge Distribution in DNA and Poly(styrenesulfonate) Aqueous Solutions. *Macromolecules* **1997**, 30 (9), 2671–2684.
- (24) Zhang, Y.; Douglas, J. F.; Ermi, B. D.; Amis, E. J. Influence of counterion valency on the scattering properties of highly charged polyelectrolyte solutions. *J. Chem. Phys.* **2001**, *114* (7), 3299–3313.
- (25) Prabhu, V.; Muthukumar, M.; Wignall, G. D.; Melnichenko, Y. B. Polyelectrolyte chain dimensions and concentration fluctuations near phase boundaries. *J. Chem. Phys.* **2003**, *119* (7), 4085–4098.
- (26) Boué, F.; Cotton, J.; Lapp, A.; Jannink, G. A direct measurement of the polyion conformation in aqueous solutions at different temperatures. Small angle neutron scattering of PSSNa using zero average and full contrast. *J. Chem. Phys.* **1994**, *101* (3), 2562–2568.

- (27) Combet, J.; Lorchat, P.; Rawiso, M. Salt-free aqueous solutions of polyelectrolytes: Small angle X-ray and neutron scattering characterization. *Eur. Phys. J. Spec. Top.* **2012**, 213 (1), 243–265.
- (28) Dubois, E.; Boué, F. Conformation of poly (styrenesulfonate) polyions in the presence of multivalent ions: small-angle neutron scattering experiments. *Macromolecules* **2001**, *34* (11), 3684–3697.
- (29) Takahashi, Y.; Matsumoto, N.; Iio, S.; Kondo, H.; Noda, I.; Imai, M.; Matsushita, Y. Concentration dependence of radius of gyration of sodium poly (styrenesulfonate) over a wide range of concentration studied by small-angle neutron scattering. *Langmuir* 1999, 15 (12), 4120–4122.
- (30) Nierlich, M.; Boué, F.; Lapp, A.; Oberthur, R. Radius of gyration of a polyion in salt free polyelectrolyte solutions measured by SANS. *J. Phys. (Paris)* **1985**, *46* (4), 649–655.
- (31) Jacobs, M.; Lopez, C. G.; Dobrynin, A. V. Quantifying the Effect of Multivalent Ions in Polyelectrolyte Solutions. *Macromolecules* **2021**, *54* (20), 9577–9586.
- (32) Lopez, C. G. Scaling and Entanglement Properties of Neutral and Sulfonated Polystyrene. *Macromolecules* **2019**, 52 (23), 9409–9415.
- (33) Han, A.; Colby, R. H. Rheology of entangled polyelectrolyte solutions. *Macromolecules* **2021**, *54* (3), 1375–1387.
- (34) Lopez, C. G. Entanglement Properties of Polyelectrolytes in Salt-Free and Excess-Salt Solutions. *ACS Macro Lett.* **2019**, 8 (8), 979–983.
- (35) Yashiro, J.; Hagino, R.; Sato, S.; Norisuye, T. Chain stiffness and excluded-volume effects in polyelectrolyte solutions: characterization of sodium poly (2-acrylamido-2-methylpropanesulfonate) in aqueous sodium chloride. *Polym. J.* **2006**, *38* (1), 57–63.
- (36) Hayashi, K.; Tsutsumi, K.; Norisuye, T.; Teramoto, A. Electrostatic contributions to chain stiffness and excluded-volume effects in sodium hyaluronate solutions. *Polym. J.* **1996**, 28 (10), 922–928
- (37) Tsutsumi, K.; Norisuye, T. Excluded-volume effects in sodium hyaluronate solutions revisited. *Polym. J.* **1998**, 30 (4), 345–349.
- (38) Di Cola, E.; Plucktaveesak, N.; Waigh, T.; Colby, R.; Tan, J.; Pyckhout-Hintzen, W.; Heenan, R. Structure and dynamics in aqueous solutions of amphiphilic sodium maleate-containing alternating copolymers. *Macromolecules* **2004**, *37* (22), 8457–8465.
- (39) Di Cola, E.; Waigh, T. A.; Colby, R. H. Dynamic light scattering and rheology studies of aqueous solutions of amphiphilic sodium maleate containing copolymers. *J. Polym. Sci., Part B: Polym. Phys.* **2007**, 45 (7), 774–785.
- (40) Boris, D. C.; Colby, R. H. Rheology of Sulfonated Polystyrene Solutions. *Macromolecules* **1998**, *31* (17), 5746–5755.
- (41) Nierlich, M.; Williams, C.; Boué, F.; Cotton, J.; Daoud, M.; Famoux, B.; Jannink, G.; Picot, C.; Moan, M.; Wolff, C. Small angle neutron scattering by semi-dilute solutions of polyelectrolyte. *J. Phys.* (*Paris*) 1979, 40 (7), 701–704.
- (42) Slim, A. H.; Shi, W. H.; Safi Samghabadi, F.; Faraone, A.; Marciel, A. B.; Poling-Skutvik, R.; Conrad, J. C. Electrostatic Repulsion Slows Relaxations of Polyelectrolytes in Semidilute Solutions. *ACS Macro Lett.* **2022**, *11*, 854–860.
- (43) Ise, N.; Okubo, T.; Kunugi, S.; Matsuoka, H.; Yamamoto, K.; Ishii, Y. "Ordered" structure in dilute solutions of sodium polystyrenesulfonates as studied by small-angle x-ray scattering. *J. Chem. Phys.* **1984**, *81* (7), 3294–3306.
- (44) Drifford, M.; Dalbiez, J. P. Effect of salt on sodium polystyrene sulfonate measured by light scattering. *Biopolymers* **1985**, 24 (8), 1501–1514.
- (45) Cohen, J.; Priel, Z.; Rabin, Y. Viscosity of dilute polyelectrolyte solutions. *J. Chem. Phys.* **1988**, *88* (11), 7111–7116.
- (46) Dobrynin, A. V.; Colby, R. H.; Rubinstein, M. Scaling theory of polyelectrolyte solutions. *Macromolecules* **1995**, 28 (6), 1859–1871.
- (47) Colby, R. H. Structure and linear viscoelasticity of flexible polymer solutions: comparison of polyelectrolyte and neutral polymer solutions. *Rheol. Acta* **2010**, *49* (5), 425–442.

- (48) Muthukumar, M. Double screening in polyelectrolyte solutions: Limiting laws and crossover formulas. *J. Chem. Phys.* **1996**, *105* (12), 5183–5199.
- (49) Chen, G.; Perazzo, A.; Stone, H. A. Influence of salt on the viscosity of polyelectrolyte solutions. *Phys. Rev. Lett.* **2020**, *124* (17), 177801.
- (50) Chen, G.; Perazzo, A.; Stone, H. A. Electrostatics, conformation, and rheology of unentangled semidilute polyelectrolyte solutions. *J. Rheol.* **2021**, 65 (4), 507–526.
- (51) Sayko, R.; Jacobs, M.; Dobrynin, A. V. Universality in Solution Properties of Polymers in Ionic Liquids. *ACS Appl. Polym. Mater.* **2022**, *4* (3), 1966–1973.
- (52) Sayko, R.; Jacobs, M.; Dobrynin, A. V. Quantifying Properties of Polysaccharide Solutions. ACS Polym. Au 2021, 1 (3), 196–205.
- (53) Dobrynin, A. V.; Jacobs, M.; Sayko, R. Scaling of polymer solutions as a quantitative tool. *Macromolecules* **2021**, *54* (5), 2288–2295.
- (54) Ise, N.; Okubo, T. Partial molal volume of polyelectrolytes. *J. Am. Chem. Soc.* **1968**, *90* (17), 4527–4533.
- (55) Kniewske, R.; Kulicke, W. M. Study on the molecular weight dependence of dilute solution properties of narrowly distributed polystyrene in toluene and in the unperturbed state. *Makromol. Chem.* 1983, 184 (10), 2173–2186.
- (56) Briscoe, B. J.; Luckham, P. F.; Ren, S. R. An assessment of a rolling-ball viscometer for studying non-Newtonian fluids. *Colloids Surf.* **1992**, *62* (1), 153–162.
- (57) Rubinstein, M.; Colby, R. H. Polymer Physics; Oxford University Press, 2003.
- (58) de Gennes, P. G.; Pincus, P.; Brochard, F.; Velasco, R. M. Remarks on polyelectrolyte conformation. *J. Phys.* (*Paris*) **1976**, *37*, 1461–1476.
- (59) Dobrynin, A. V. Polyelectrolyte Solutions and Gels. In *Oxford Handbook of Soft Matter*; Terentjev, E., Weitz, D., Eds.; Oxford University Press, 2015; pp 269–344.
- (60) de Gennes, P. G. Dynamics of entangled polymer solutions. I. The Rouse model. *Macromolecules* **1976**, 9 (4), 587–593.
- (61) de Gennes, P. G. Dynamics of entangled polymer solutions. II. Inclusion of hydrodynamic interactions. *Macromolecules* **1976**, 9 (4), 594–598.
- (62) de Gennes, P. G. Scaling Concepts in Polymer Physics; Cornell University Press, 1979.
- (63) Doi, M.; Edwards, S. F. The Theory of Polymer Dynamics; Clarendon Press Oxford, 1986.
- (64) Kavassalis, T. A.; Noolandi, J. New view of entanglements in dense polymer systems. *Phys. Rev. Lett.* **1987**, *59* (23), 2674–2677.
- (65) Kavassalis, T. A.; Noolandi, J. Entanglement scaling in polymer melts and solutions. *Macromolecules* **1989**, 22 (6), 2709–2720.
- (66) Fetters, L.; Hadjichristidis, N.; Lindner, J.; Mays, J. Molecular Weight Dependence of Hydrodynamic and Thermodynamic Properties for Well-Defined Linear Polymers in Solution. *J. Phys. Chem. Ref. Data* **1994**, 23 (4), 619–640.
- (67) Lopez, C. G.; Horkay, F.; Schweins, R.; Richtering, W. Solution properties of polyelectrolytes with divalent counterions. *Macromolecules* **2021**, 54 (22), 10583–10593.
- (68) Lopez, C. G.; Richtering, W. Viscosity of Semidilute and Concentrated Nonentangled Flexible Polyelectrolytes in Salt-Free Solution. *J. Phys. Chem. B* **2019**, *123* (26), 5626–5634.
- (69) Kestin, J.; Khalifa, H. E.; Correia, R. J. Tables of the dynamic and kinematic viscosity of aqueous NaCl solutions in the temperature range 20–150 °C and the pressure range 0.1–35 MPa. *J. Phys. Chem. Ref. Data* **1981**, *10* (1), 71–88.
- (70) Fuoss, R. M. Polyelectrolytes. Science 1948, 108 (2812), 545-550.
- (71) Fuoss, R. M. Viscosity function for polyelectrolytes. *J. Polym. Sci.* **1948**, *3*, 603–604.
- (72) Kaji, K.; Urakawa, H.; Kanaya, T.; Kitamaru, R. Phase diagram of polyelectrolyte solutions. *J. Phys. (Paris)* **1988**, 49 (6), 993–1000.
- (73) Combet, J.; Rawiso, M.; Rochas, C.; Hoffmann, S.; Boué, F. Structure of polyelectrolytes with mixed monovalent and divalent

counterions: SAXS measurements and Poisson-Boltzmann analysis. *Macromolecules* **2011**, 44 (8), 3039–3052.

- (74) Bordi, F.; Cametti, C.; Colby, R. Dielectric spectroscopy and conductivity of polyelectrolyte solutions. *J. Phys.: Condens. Matter* **2004**, *16* (49), R1423.
- (75) Colby, R. H.; Boris, D. C.; Krause, W. E.; Tan, J. S. Polyelectrolyte conductivity. *J. Polym. Sci., Part B: Polym. Phys.* **1997**, 35 (17), 2951–2960.
- (76) Manning, G. S. Limiting laws and counterion condensation in polyelectrolyte solutions I. Colligative properties. *J. Chem. Phys.* **1969**, *51* (3), 924–933.
- (77) Manning, G. S. Polyelectrolytes. Annu. Rev. Phys. Chem. 1972, 23 (1), 117–140.

# **□** Recommended by ACS

# Viscosity of Sodium Polystyrenesulfonate with Cetyltrimethylammonium Bromide in the Mixture of Methanol and Water

Ajaya Bhattarai and Bijan Das

JULY 28, 2023

THE JOURNAL OF PHYSICAL CHEMISTRY B

READ 🗹

# **Concentration Regimes for Extensional Relaxation Times of Unentangled Polymer Solutions**

Diego D. Soetrisno, Jacinta C. Conrad, et al.

JUNE 27, 2023

MACROMOLECULES

READ 🗹

# Influence of Chain Entanglement on Rheological and Mechanical Behaviors of Polymerized Ionic Liquids

Gang Liu, Guangxian Li, et al.

MARCH 31, 2023 MACROMOLECULES

READ 🗹

# **Effect of a Cationic Polymer on the Rheology of Cement Pastes Containing Na-Bentonite**

Pengpeng Wen, Baicun Zheng, et al.

FEBRUARY 09, 2023

LANGMUIR

READ 🗹

Get More Suggestions >